

Curvature-Based Control for Low-Inertia Systems

Francesco Sanniti, *Member, IEEE*, Georgios Tzounas, *Member, IEEE*, Roberto Benato, *Senior Member, IEEE*, Federico Milano, *Fellow, IEEE*

Abstract—This letter proposes a simple and inexpensive control of distributed energy resources aimed at improving the power system dynamic performance. The rationale behind the proposed control relies on a recent interpretation of the frequency in the differential geometry framework. A comparison with well-established controls in terms of eigensensitivity and time-domain performance is carried out to show the effectiveness of the proposed control.

Index Terms—Differential geometry, Power Oscillation Damper (POD), Participation Factor (PF), Low-inertia Systems.

I. INTRODUCTION

In the last decades, power systems have undergone a massive replacement of conventional synchronous generators by power converter-based resources. This has led to significant changes of the dynamic performance and stability properties of the system [1]. For this reason, significant efforts have been made, by both industry and academia, to find reliable and robust control solutions for this unprecedented scenario.

A promising approach consists in taking advantage of the fast control capabilities of inverter-based generation and interfaces to improve the system stability. For example, in [2], the synthetic inertia and droop coefficients of Distributed Energy Resources (DERs) are designed to meet time-domain performance objectives of frequency overshoot and steady-state regulation. In [3], a control framework is proposed for the provision of ancillary services by aggregated DERs. Moreover, a multi-sensitivity control approach for VSC-HVDC links and FACTS devices is described in [4].

Some recent studies have felt the need for the definition of new control signals that improve the dynamic performance of low-inertia systems, e.g. see [5]–[7]. This letter proposes a control scheme based on a novel signal that stems from the theory of the differential geometry. In particular, the starting point is a geometrical interpretation of electric circuits recently proposed by the second and fourth authors [8]. According to this interpretation, the concept of *curvature* appears to provide relevant information on the local transient behavior of electrical quantities. A curvature based-control is a well-established concept for different applications, such as continuum robotics [9]. In this letter, the curvature control is applied to power

systems, by adopting the curvature as an input signal for an auxiliary control scheme applied to DERs, and its performance is compared with the ones of conventional input signals, such as frequency and voltage magnitude.

II. PROPOSED CONTROL SCHEME

The starting point of the proposed control approach is the definition of curvature in an electric circuit as recently discussed in [8]. The main idea of [8] is that the vector of the voltage, \mathbf{v} , can be thought as the time derivative (or velocity) of a space curve. This curve is, in effect, the magnetic flux, as it descends from Faraday's law. Assuming this formal equivalence, namely voltage-velocity, the *curvature* of the three-phase magnetic flux is defined as:

$$\kappa = \left| \frac{\mathbf{v}}{v} \times \frac{\mathbf{v}'}{v^2} \right|, \quad (1)$$

where \mathbf{v}' is the time derivative of \mathbf{v} , \times denotes the vector product, and $v = \sqrt{\mathbf{v} \cdot \mathbf{v}}$ is the voltage magnitude, with \cdot being the scalar product of two vectors. The Park transform of a time-varying balanced three-phase voltage vector \mathbf{v} leads to [8]:

$$\kappa = \frac{\omega}{v}, \quad (2)$$

where

$$\omega = \omega_o + \frac{v'_d v_d - v'_q v_q}{v^2}, \quad (3)$$

is the well-known instantaneous angular frequency of the voltage. Note that (2) holds true also in general (e.g., unbalanced and/or non-sinusoidal multi-phase systems) but in that case ω assumes the meaning of the module of the geometric frequency [10], which does not always coincide with the instantaneous frequency.

This letter proposes to use (2) in auxiliary control loops of DERs to improve the dynamic performance of power systems. With this aim, we use an auxiliary device, i.e. a standard Power Oscillation Damper (POD) (see, e.g., [11]), whose output is added to the voltage reference of the DER voltage control. This controller allows testing the proposed scheme in transient conditions and has been chosen for its effectiveness to damp oscillatory modes. The control diagram of the POD model is shown in Fig. 1. The model consists of a low-pass filter on the input signal u , a washout filter with gain K_w and time constant T_w , and a double lead lag filter with a windup limiter on the output $v_{\text{POD}}^{\text{ref}}$. Note that the washout filter makes the POD sensitive to the rate of change of the input signal, not the value of the input signal itself. The POD is thus inactive for constant values of the input signal.

An estimation of the curvature can be easily obtained in practice, as κ is the ratio of two quantities commonly

Francesco Sanniti and Roberto Benato are with the Department of Industrial Engineering, University of Padova, 35122, Padova, Italy. (e-mails: francesco.sanniti@phd.unipd.it, roberto.benato@unipd.it)

Georgios Tzounas is with the Power System Laboratory, ETH Zürich, 8092 Zürich, Switzerland. (e-mail: georgios.tzounas@eeh.ee.ethz.ch)

Federico Milano is with the School of Electrical & Electronic Engineering, University College Dublin, D04V1W8, Dublin, Ireland. (e-mail: federico.milano@ucd.ie)

This work is supported by the Italian Ministry of Education by funding F. Sanniti under the framework of the 35th PhD Programme; and by Sustainable Energy Authority of Ireland by funding F. Milano under project FRESLIPS, Grant No. RDD/00681.

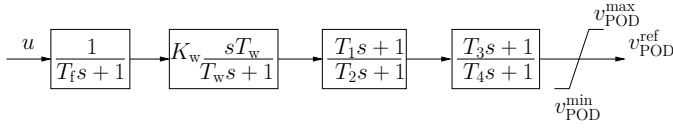


Fig. 1. Control diagram of the POD.

measured at network buses, namely angular frequency and voltage magnitude.

The performance of the proposed curvature-based control under varying operating conditions can be assessed through non-linear time-domain simulations.

Yet, a qualitative appraisal of the performance of a signal for control purposes can be obtained through modal participation analysis of the linearized system [12]. In particular, we are interested in evaluating the Participation Factor (PF) that links κ with the dynamic modes of the system and compare such a PF with those of standard signals utilized in power system control loops, such as the frequency and the voltage magnitude. With this aim, we first define the expression of the PF of a generic signal, say z , defined as:

$$z = x_j / y_k, \quad (4)$$

where x_j is the j -th state variable and y_k is the k -th algebraic variable of a set of non-linear Differential-Algebraic Equations (DAEs). The participation matrix $\mathbf{P}_x \in \mathbb{R}^{n \times n}$ for a linearized system with n state variables, can be expressed as [13]:

$$\mathbf{P}_x = |\Psi|^T \circ |\Phi|, \quad (5)$$

where \circ denotes the element-wise multiplication, and \top denotes the matrix transpose. In (5), Ψ and Φ are matrices formed with the left and the right eigenvectors of the state matrix of the system, calculated at a given equilibrium point.

An approach to determine the PFs of algebraic variables in the dynamic modes of a power system is given in [13]:

$$\mathbf{P}_y = -\mathbf{g}_y^{-1} \mathbf{g}_x \mathbf{P}_x, \quad (6)$$

where \mathbf{g}_y and \mathbf{g}_x are the Jacobian matrices of the algebraic equations of the explicit non-linear DAE system evaluated at $(\mathbf{x}_o, \mathbf{y}_o)$, with n differential and m algebraic equations.

Differentiation of (4) around $(x_{j,o}, y_{k,o})$ yields:

$$\Delta z = \frac{1}{y_{k,o}} \Delta x_j - \frac{x_{j,o}}{y_{k,o}^2} \Delta y_k, \quad (7)$$

and, exploiting the superposition principle for linear systems on (7), the PF $p_{z(i)}$ of the signal z on the i -th mode is:

$$p_{z(i)} = \frac{1}{y_{k,o}} p_{x(j,i)} - \frac{x_{j,o}}{y_{k,o}^2} p_{y(k,i)}. \quad (8)$$

Equation (6) indicates that $p_{y(j,i)}$ depends on the network parameters and topology through the k -th row of the matrix \mathbf{g}_y^{-1} and on the matrix \mathbf{g}_x . By assuming $x_{j,o}, y_{k,o} \approx 1$ pu (which is reasonable if one sets $z = \kappa$, $x_j = \omega$ and $y_k = v$) and by knowing that $p_{x(j,i)} > 0 \forall p_x \in \mathbb{R}^{n \times n}$, one obtains:

$$p_{z(i)} > p_{x(k,i)}, p_{y(k,i)} \quad \forall p_y \in \mathbb{R}^{m \times n} : p_y < 0. \quad (9)$$

This condition is utilized in the case study presented below.

III. CASE STUDY

In this section, the IEEE 39-bus benchmark system is utilized to illustrate the dynamic performance of the proposed curvature-based control. All simulation results are obtained with the software tool Dome [14].

The system is modified to emulate a low-inertia system. This helps appreciating the dynamic effect of the proposed control. In particular, a converter-based DER is added at every generation bus. The DER model employed and its primary controllers are described in [6]. At generation buses, the power share of DERs is imposed through a parameter $\gamma \in [0, 1]$, which scales the capacity of both synchronous machines and DERs to ensure that the total generation capacity S_n remains constant:

$$S_n^{\text{DER}} = S_n \gamma, \quad S_n^{\text{Syn}} = S_n (1 - \gamma). \quad (10)$$

In the simulations discussed below, we set $\gamma = 0.7$. Finally, loads are represented by an exponential model that depends on both voltage and frequency, see [15].

The DER models and the controllers utilised in this case study include current limiters and other windup and anti-windup limiters. Moreover, in one scenario of the case study, we have considered a three-phase fault that is cleared by triggering a line and, hence, by changing the topology of the grid. The system model, thus, properly takes into account the dynamic couplings among DERs and other devices and controllers in the system.

Table I shows the five most poorly damped eigenvalues of the modified IEEE 39-bus system and the corresponding PFs in these modes of the frequency ω_h , the voltage v_h , and the curvature κ_h . The quantities ω_h and v_h are measured at the h -th bus, where h is the index of the bus where the device with the state variable participating the most in each mode of Table I is located. The PF of κ_h is calculated according to (8). We observe that the results given in Table I always satisfy condition (9), with κ_h having the highest PF for the five most critical eigenvalues. That is, the small-signal analysis indicates that κ_h is more effective than ω_h and v_h in suppressing the most critical modes of the system.

TABLE I
PFs FOR SYSTEM CRITICAL MODES.

Mode	x-dom.	p		
		ω_h	v_h	$\kappa_h = \omega_h / v_h$
$-1.169 \pm j12.573$	$\omega_{\text{Syn } 1}$	0.87e-5	-0.22e-5	1.05e-5
$-1.447 \pm j24.050$	$\omega_{\text{Syn } 3}$	2.62e-3	-2.93e-3	5.70e-3
$-1.947 \pm j27.404$	$\omega_{\text{Syn } 4}$	1.02e-4	-2.49e-4	3.52e-4
$-1.951 \pm j29.345$	$\omega_{\text{Syn } 8}$	1.54e-4	-0.61e-4	2.07e-4
$-1.998 \pm j23.490$	$\omega_{\text{Syn } 9}$	6.01e-2	-0.52e-2	6.35e-2

In non-linear time-domain simulations, we compare the base-case system with and without PODs and for the following three different input signals u :

- bus frequency ω_h ;
- bus voltage magnitude v_h ;
- curvature $\kappa_h = \omega_h / v_h$.

A POD is added to each DER connected to the bus h . For fair comparison, the tuning of the PODs is optimized for each

signal u according to the method of residues [16], whereas gains K_w are set using a trial and error procedure to realize the maximum damping for each POD and for each input signal. Table II summarizes the results of the tuning.

TABLE II
PARAMETERS OF THE POD TUNED WITH THE METHOD OF RESIDUES.

h -th POD	signal	T_f	K_w	T_w	T_1	T_2	T_3	T_4
#1	ω_1	0	8	3.4	0.28	0.01	0.0	0.0
	v_1	0.2	-4	5	0.037	0.17	0.0	0.0
	κ_1	0.2	4	3.4	0.5	0.006	0.0	0.0
#3	ω_3	0	8	2.7	0.22	0.01	0.0	0.0
	v_3	0.2	-3	2.6	0.1	0.017	0.0	0.0
	κ_3	0.2	4	2.7	0.12	0.014	0.12	0.014
#4	ω_4	0	8	2.3	0.11	0.01	0.0	0.0
	v_4	0.2	-3	2.3	0.027	0.05	0.0	0.0
	κ_4	0.2	2	2.3	0.15	0.01	0.15	0.01
#8	ω_8	0	5	2.2	0.003	0.36	0.003	0.36
	v_8	0.2	-3	2.1	0.01	0.09	0.0	0.0
	κ_8	0.2	6	2.2	0.6	0.002	0.0	0.0
#9	ω_9	0	5	2.7	0.09	0.02	0.0	0.0
	v_9	0.2	-3	2.7	0.02	0.08	0.0	0.0
	κ_9	0.2	6	2.7	0.4	0.004	0.0	0.0

We consider two contingencies: (i) the distributed outage of 24% of the load consumption; and (ii) a short circuit at bus 12 cleared after 0.1 s. The simulation results for the load outage and for the short circuit are shown respectively in Figs. 2 - 5. The results show the transient behavior of frequency and voltage, as well as the active power injected by DERs and Synchronous Generators (SGs) to the grid.

The PODs driven by the curvature signal restore the stationary condition faster and with higher damping than the PODs that utilize the voltage frequency and magnitude. This result is consistent with the small-signal analysis above.

It is relevant to note that the proposed control does not increase the effort, namely the active power generation, of the DERs or of the synchronous generators. Moreover, note that, in the case of loss of load, the PODs with conventional input signals cannot remove oscillations and in the scenario for which the input signal of the POD is the bus voltage magnitude, the system becomes unstable (undamped oscillations). In all scenarios, the proposed curvature-based POD control is able to properly damp the oscillations, also resulting in lower power oscillations by the machines and DERs.

IV. CONCLUSIONS

This letter uses as starting point a recently proposed geometric interpretation of the transient behavior of electric quantities in ac power systems. The effectiveness of this approach is confirmed by the eigensensitivity analysis and the evaluation of the PFs, and by a time-domain simulation, both performed on a low-inertia system. Simulation results show that a control based on the curvature is more effective than the same control driven by the voltage magnitude or frequency.

Besides being effective, the proposed control is also simple and inexpensive to implement. It is simple, as the proposed controller is a conventional POD, which effectively has the same implementation as a power system stabilizer, and it has

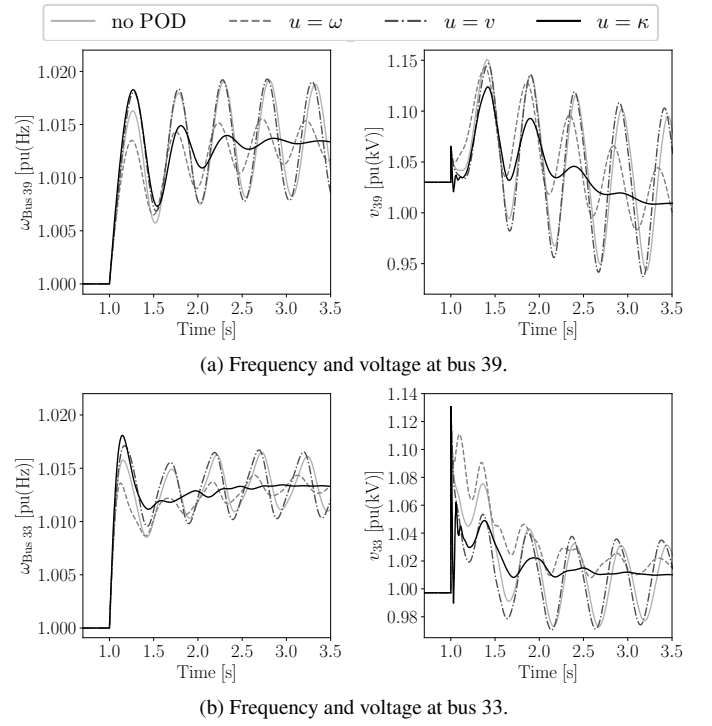


Fig. 2. Transient response following the outage of 24% of the load.

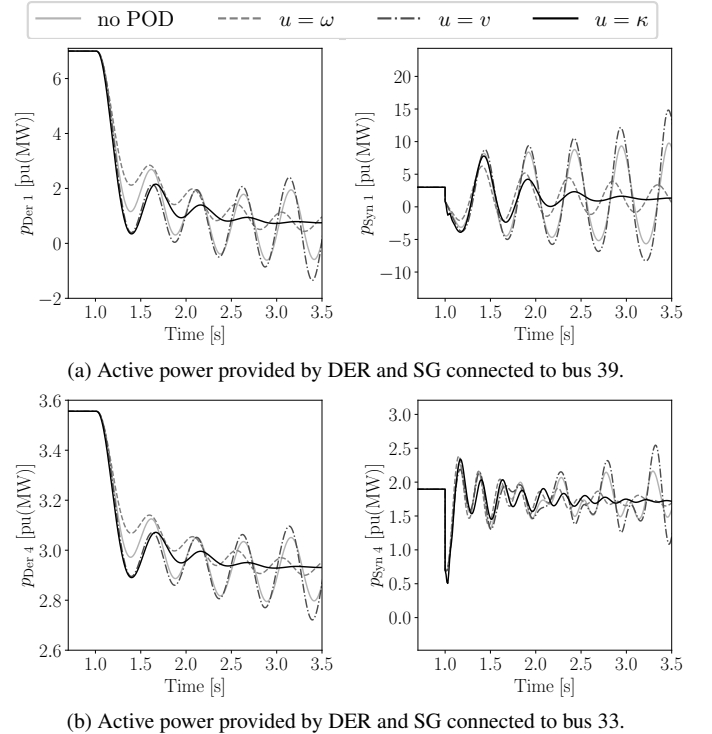


Fig. 3. Transient response following the outage of 24% of the load.

been widely discussed and utilized in the literature. It is inexpensive, as a POD can be implemented with a microcontroller, which has a cost of the order of US\$ 100.

Moreover, the proposed control does not require to measure remote signals and hence does not require an *ad hoc* communication system, nor it requires to measure quantities that require expensive hardware. The curvature, in fact, is obtained

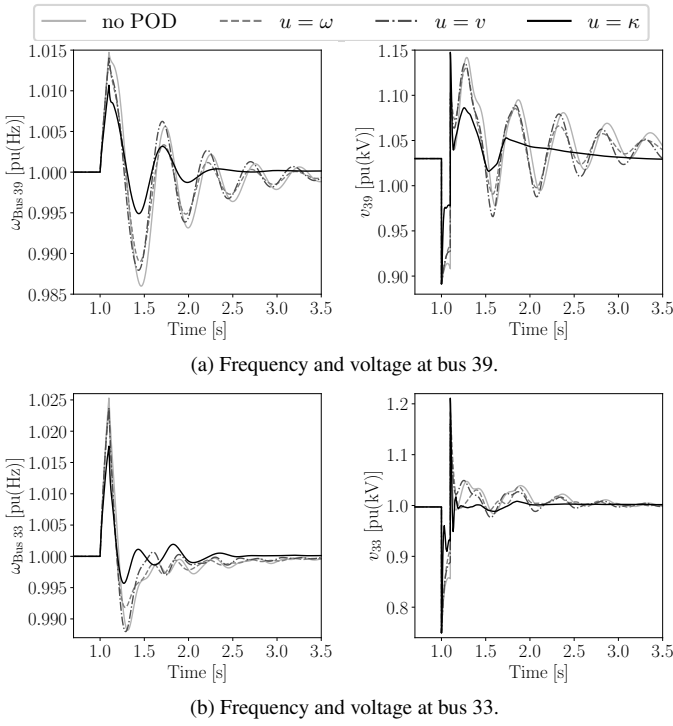


Fig. 4. Transient response following a fault at bus 12 cleared after 0.1 s.

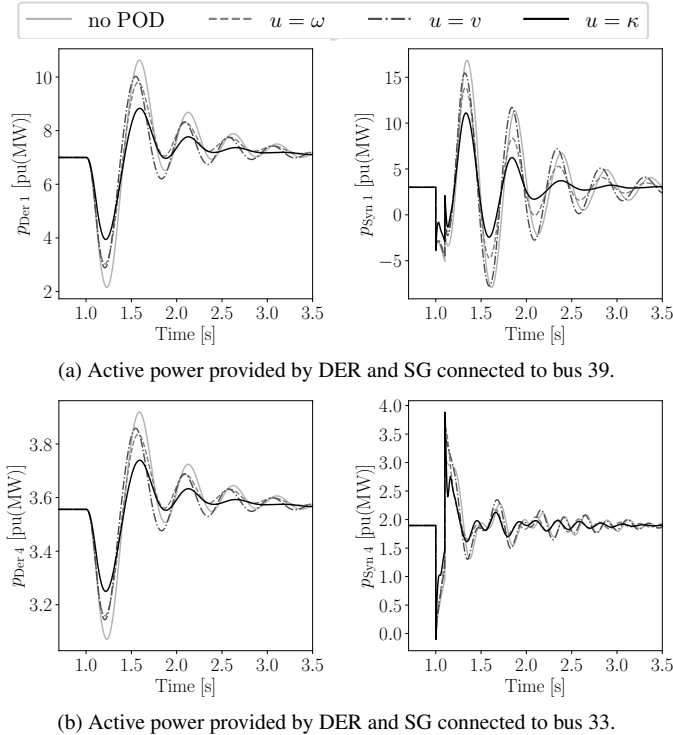


Fig. 5. Transient response following a fault at bus 12 cleared after 0.1 s.

by simply dividing the frequency and the magnitude of the bus voltage at the point of connection of the DER with the grid. These measurements are needed for the conventional control of DERs, and hence the estimation of the curvature does not suppose additional costs.

REFERENCES

- [1] F. Milano, F. Dörfler, G. Hug, D. J. Hill, and G. Verbič, "Foundations and challenges of low-inertia systems (invited paper)," in *2018 Power Systems Computation Conference (PSCC)*, 2018, pp. 1–25.
- [2] S. S. Guggilam *et al.*, "Optimizing DER participation in inertial and primary-frequency response," *IEEE Trans. on Power Systems*, vol. 33, no. 5, pp. 5194–5205, 2018.
- [3] E. Dall'Anese *et al.*, "Optimal regulation of virtual power plants," *IEEE Trans. on Power Systems*, vol. 33, no. 2, pp. 1868–1881, 2018.
- [4] B. Chaudhuri *et al.*, "Mixed-sensitivity approach to H_∞ control of power system oscillations employing multiple FACTS devices," *IEEE Trans. on Power Systems*, vol. 18, no. 3, pp. 1149–1156, 2003.
- [5] W. Zhong, G. Tzounas, and F. Milano, "Improving the power system dynamic response through a combined voltage-frequency control of distributed energy resources," *IEEE Trans. on Power Systems*, pp. 1–1, 2022.
- [6] G. Tzounas and F. Milano, "Improving the frequency response of DERs through voltage feedback," in *2021 IEEE Power Energy Society General Meeting (PESGM)*, 2021, pp. 1–5.
- [7] Y. Shen, W. Yao, J. Wen, H. He, and W. Chen, "Adaptive supplementary damping control of vsc-hvdc for interarea oscillation using grhdp," *IEEE Trans. on Power Systems*, vol. 33, no. 2, pp. 1777–1789, 2018.
- [8] F. Milano, G. Tzounas, I. Dassios, and T. Kërçi, "Applications of the Frenet frame to electric circuits," *IEEE Trans. on Circuits and Systems I: Regular Papers*, pp. 1–13, 2021.
- [9] I. Robert J. Webster and B. A. Jones, "Design and kinematic modeling of constant curvature continuum robots: A review," *The International Journal of Robotics Research*, vol. 29, no. 13, pp. 1661–1683, 2010.
- [10] F. Milano, "A geometrical interpretation of frequency," *IEEE Trans. on Power Systems*, vol. 37, no. 1, pp. 816–819, 2022.
- [11] D. P. Ke and C. Y. Chung, "An inter-area mode oriented pole-shifting method with coordination of control efforts for robust tuning of power oscillation damping controllers," *IEEE Trans. on Power Systems*, vol. 27, no. 3, pp. 1422–1432, 2012.
- [12] B. P. Padhy *et al.*, "A coherency-based approach for signal selection for wide area stabilizing control in power systems," *IEEE Systems Journal*, vol. 7, no. 4, pp. 807–816, 2013.
- [13] G. Tzounas *et al.*, "Modal participation factors of algebraic variables," *IEEE Trans. on Power Systems*, vol. 35, no. 1, pp. 742–750, 2020.
- [14] F. Milano, "A Python-based software tool for power system analysis," in *IEEE PES General Meeting*, 2013, pp. 1–5.
- [15] G. L. Berg, "Power system load representation," *Proceedings of IEE*, vol. 120, pp. 344–348, 1973.
- [16] Milano, F., Dassios, I., Liu, M., and Tzounas, G., *Eigenvalue Problems in Power Systems (1st ed.)*. CRC Press, 2021.